Shear Behavior of Engineered Cementitious Composite Structural Members

Sebastian Varela[1], M. 'Saiid' Saiidi[2]

[1] PhD Student and Graduate Research Assistant, Dept. of Civil and Environmental Engineering, University of Nevada, Reno NV, USA
[2] Professor, Dept. of Civil and Environmental Engineering, University of Nevada, Reno NV, USA

ABSTRACT: Although the ECC material (engineered cementitious composite) possesses features that make it suitable for structural applications, there is a lack of an adequate model to predict its shear strength. This parameter is necessary to estimate the capacity of structural elements under critical loading conditions. An experimental program on the shear strength of ECC is underway at the University of Nevada, Reno. A total of 40 shear tests are being conducted on simply supported ECC beam specimens subjected to point loading. The main test variables include the compressive strength of ECC, the shear span, and the longitudinal reinforcement ratio in the beams. This paper presents a summary of the state-of-the-art, the experimental testing program, the test results, and the preliminary assessment of the ability of existing equations to predict the shear strength of ECC.

1   INTRODUCTION

Engineered cementitious composite (ECC) is a type of high performance fiber reinforced cementitious material (HPFRC) that possesses a series of features that make it desirable for structural applications. Naaman and Reindhart (2006) recognized the typical response of HPFRC under tensile loading as one characterized first by a steep initial elastic portion, up to the point in which the first crack occurs. Subsequently there is a post-elastic ascending branch (strain hardening) where multiple cracks develop within the material and the fibers bridge inside the cracks, followed by a descending branch up to rupture. This behavior gives the composite a high tensile strength and ductility when compared to conventional concrete and makes ECC a suitable material for the concrete used in the zones of high ductility demand of structural elements.

Fischer & Li (2002) conducted cyclic tests on steel-reinforced rectangular columns made of ECC and concrete. Even though the reinforced concrete (RC) test column had a fair amount of transverse reinforcement and the ECC column had no transverse reinforcement, they observed that the extent of apparent damage, dissipated energy and load carrying capacity of the column was greatly improved due to the ductile response of ECC. Saiidi et al. (2009) tested 1/5 scale cantilever bridge columns under cyclic loading. In order to minimize cost, the columns were constructed using ECC and superelastic Nickel-Titanium (NiTi) only in the plastic hinge zone, while the upper part was made of conventional RC. Among the main conclusions of this study is the fact that ECC considerably reduced the damage within the columns, which could allow a bridge structure to remain serviceable even after a strong earthquake. In addition, the study by

Cruz & Saiidi (2013) shows that ECC can be used to effectively reduce the damage at the plastic hinge region of a column that is part of a bridge system subjected to earthquake loading.

Despite its aforementioned benefits, if ECC is to be employed for structural applications it is necessary to establish reliable design methodologies that would allow engineers to estimate the capacity of this material under critical loading conditions.

For most structural design scenarios, the members are dimensioned and detailed such that shear failure would not be the controlling failure mechanism of the member. This is mainly due to the brittle nature associated with such failure mechanism. Consequently, there is a need to have a reliable model to estimate the shear capacity of ECC. Surprisingly, there are only a handful of studies related to this matter, and therefore no specific shear design guidelines exist yet for ECC.

Kanakubo et al. (2007) performed tests on 16-180 mm x 280 mm PVA-ECC beams subjected to pure shear (i.e. with no bending) considering fiber volumes of 1.5% and 2.0%. These researchers found a fairly good correlation between the shear strength of the test specimens and the formula in the A-method of the Architecture Institute of Japan Design guidelines. However, they acknowledged the high uncertainty in estimating one of the factors in the formula. The study by Xu et al (2012) included tests of 15 simply supported ECC beams having PVA fibers and varying shear span ratio. An empirical formula was proposed based on their test data and then compared to data from tests on strain-softening steel fiber reinforced composites. The formula is complex and may undermine its adoptability for practical engineering applications.

In order to gather a larger number of data points to evaluate the applicability of some of the existing models to predict the shear strength of ECC and to address the need to develop a new practical and comprehensive model, an experimental study is currently being conducted at the University of Nevada, Reno. In this study, 40 shear tests are being conducted on simply supported ECC beam specimens subjected to point loading. The main test variables include the compressive strength of ECC, the shear span, and the longitudinal reinforcement ratio in the beams. Eighteen beam specimens having short shear-span ratio are tested twice, providing data for 36 combinations of variables. The beams are loaded in an asymmetric pattern. After the first test, the specimens are repaired with epoxy injection of the cracks and wrapped with carbon fiber reinforced polymer fabrics. Four additional beams with relatively large shear-span ratio are tested to study the influence of the arch action on the ECC shear behavior.

The results of this study will be used during an on-going research project at the University of Nevada, Reno whose primary objective is to develop details for detachable plastic hinge elements for precast bridge columns using innovative materials. These details will allow for assembly and disassembly of earthquake resistant bridge columns that can be recycled, thus leading to sustainable bridge designs.

2   EXPERIMENTAL PROGRAM

2.1   *Materials*

2.1.1   ECC

ECC was supplied by Fiber Matrix Inc., Sparks, Nevada. Three mixes were tailored so as to have compressive strengths of 28 MPa (4 ksi), 38.5 MPa (5.5 ksi) and 49 MPa (7 ksi). For all mixes, kuraray Kuralon RECS15 PVA fibers at a dosage of 2% by volume were used. The mix

was completed using Type I hydraulic cement, water, fly ash, silica sand, super plasticizer and a low viscosity thickener to improve workability.

2.1.2   Mild steel reinforcement

Standard ASTM A706 grade 60 reinforcing steel with a minimum yield strength of 420 MPa and rupture strength of 550 MPa (80 ksi) was used as longitudinal reinforcement in all beam specimens. In addition, specimens having large shear span ratio (*a/d*) on sets 10 and 11 (refer to Table 1) had #3 stirrups of the same steel grade.

2.1.3   Carbon Fiber Reinforced Polymer (CFRP) Fabrics

As mentioned before, 18 beam specimens are loaded in an asymmetric pattern and tested twice. After the first test, each specimen is repaired using a pressure epoxy injection inside the cracks and then wrapped with CFRP in a U-pattern (i.e. the top face of the beam is kept free). After the repair and once the epoxy and wrap have cured, the specimen is re-tested. For the wrap, Tyfo SCH-41S CFRP fabric from the Fyfe co. was used. It is a custom weave, uni-directional carbon fabric with aramid cross fibers. The carbon material is orientated in the 0 direction with aramid fibers at 90. The fabric is applied using the two-component Tyfo S Epoxy matrix. The main design criterion for the CFRP was to restore the shear strength on the damaged end of the test specimen, thus enabling the opposite end to fail in shear during the second test.

2.2   Description of test specimens

Equation 11-5 on Section 11.2.2.1 of the Building Code Requirements for Structural Concrete ACI 318-11 by the American Concrete Institute (ACI) is the basic expression for the shear strength provided by non-prestressed concrete members without web reinforcement. This equation has been adopted by concrete design codes all around the globe and it is an empirical expression based on a wide range of experimental tests gathered by the Joint ACI-ASCE Committee 326 (1962). The document by Joint Committee 326 acknowledges the shear strength of a concrete element being influenced primarily by its longitudinal reinforcement ratio, ρ, its concrete tensile strength, expressed as a function of the square root of its compressive strength, $\sqrt{f'_c}$ and the ratio between the bending moment, *M*, and the product of the internal shear force, *V* and the effective depth of the section being considered, *d*. The design equation in ACI 318-11 is then expressed as a function of the factor *B*, defined in Eq. (1):

$$B = \frac{\rho V d}{M\sqrt{f'_c}} \qquad (1)$$

In order to study the influence of these variables on the shear strength of ECC structural members, the test beam specimens were designed to have different values for the factor *B*. Table 1 shows the characteristics of all the test specimens.

Specimens belonging to sets 1-9 have 2 replicates, each tested twice for a total of 36 data points. Specimens 10 and 11 having a larger shear span and stirrups outside the shear span are tested only once, for a total of 4 data points. It is important to notice that the longitudinal reinforcement is only located at the bottom of the specimens.

2.3   Test setup and procedure

The beam specimens are being tested using a displacement-controlled hydraulic ram, as shown in Figure 1. Steel plates capable of rotating are used as supports located at the ends of the beam. The load is transferred from the ram onto a pancake load cell and then to a swivel plate acting as

a hinge preventing any moment of being transferred to the beam specimen. Strain gages are installed on each longitudinal reinforcing bar under the point of load application. These gages provide information on the rebar strain associated with the maximum bending moment in the beam.

Table 1. Characteristics of test specimens

	Set #										
	1	2	3	4	5	6	7	8	9	10	11
f'_c (MPa) =	28	38.5	38.5	38.5	49	49	28	28	28	38.5	49
b (mm) =				127				203.2		127	
h (mm) =	304.8	304.8	304.8	304.8	304.8	304.8	304.8	317.5	342.9	304.8	304.8
d (mm) =	281.0	279.4	276.2	277.8	274.6	276.2	276.2	244.3	266.5	257.2	254.2
a (mm) =	406.4	279.4	406.4	304.8	266.7	276.2	276.2	266.7	266.7	838.2	838.2
a/d =	1.4	1.0	1.5	1.1	1.0	1.0	1.0	1.1	1.0	3.3	3.3
Reinf =	3#3	2#4	2#6	3#5	2#7	3#6	3#6	4#7	4#8	2#6	2#7
A_s (mm^2) =	213.0	258.0	568.0	597.0	774.0	852.0	852.0	1548.0	2040.0	568.0	774.0
$B/1000$ =	0.06	0.10	0.15	0.20	0.27	0.29	0.37	0.44	0.58	0.07	0.09
Stirrups	-	-	-	-	-	-	-	-	-	#3@64	#3@64

The K600 Krypton camera system belonging to the George E. Brown Jr. Network for Earthquake Engineering Simulation (NEES) was used to record displacement data in each of the test specimens. The K600 is an optical motion measurement system that makes use of a camera (Figure 1, right) capable of measuring the position of multiple LED targets in space (X,Y,Z). LED targets are glued to the front face of each specimen on selected positions along its length and height. Typically, as depicted in Figure 1, six lines of LEDs are placed on each specimen: at both supports, under the point of load application, at the middle of the shear span, at the middle of the beam span, and at ¾ of the beam span. During each test, the load, ram displacement and K600 readings are recorded simultaneously at a sampling rate of 24 Hz.
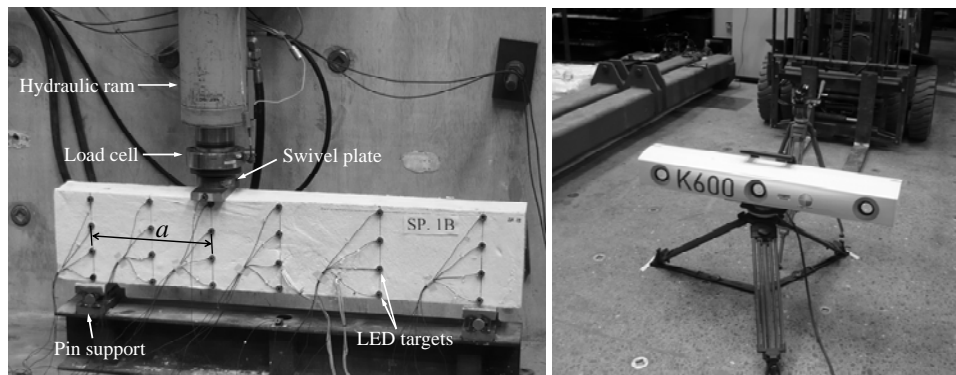

Figure 1. Test setup and K600 camera system.

During each test, the specimen is loaded continuously at a constant displacement rate of 2.54mm/min (0.1 in./min) up to failure. Additional loading following failure is performed to determine the residual capacity of each specimen.

3   PRELIMINARY TEST RESULTS AND OBSERVATIONS

By the time of the submission of this paper, a total of 19 tests have been conducted. However, only the results for tests 1A to 1D and 2A to 2D are presented herein. Note that each 'virgin' test specimen is labeled as A or B and once repaired they are labeled as C and D, respectively.
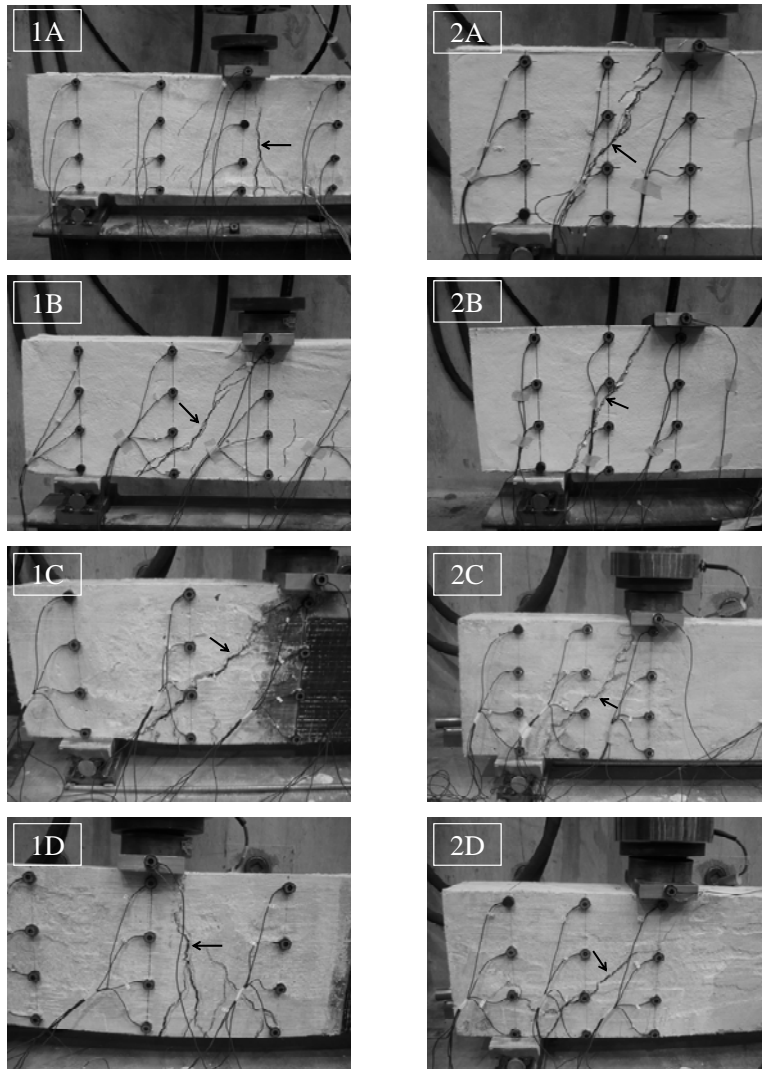
3.1   Failure modes

Figure 2. Failure mode of test specimens.

Figure 2 depicts the failure mode of the group 1 and 2 specimens. An arrow is used to indicate the principal crack. As can be seen in Figure 2, the typical failure mode consists on a series of diagonal cracks that extend over the entire height of the beam connecting the left edge of the loading plate and the right edge of the support plate. However, flexural failure was observed in 1A and 1D, mainly caused by their high shear strength and relatively low longitudinal reinforcement ratio.

3.2 *Force-displacement behavior*

Table 2 and Figure 3 show the test results for specimens 1A-D and 2A-D. The yield and ultimate displacements, Δ_y and Δ_u, as well as the elastic and plastic stiffnesses k_e and k_p shown in Table 2 are defined based on a bi-linear curve fit to the experimental data. Percent flexural and shear contributions to each of the aforementioned displacements are also shown in Table 2. Shear displacements were calculated by subtracting the flexural displacements (computed based on experimental curvature measurements) from the total measured displacements.

Note that the curves presented in Figure 3 correspond to the total load measured by the load cell, whereas the force of interest is the internal shear force in the beam, shown in Table 2.

Table 2. Test results

	Test #							
	1A	1B	1C	1D	2A	2B	2C	2D
Δ_y (mm) =	3.2	3.3	1.8	2.1	2.4	1.9	2.0	2.1
% flexure=	72.7%	79.5%	*	91.4%	75.5%	90.7%	87.3%	78.6%
% shear=	27.3%	20.5%	*	8.6%	24.5%	9.3%	12.7%	21.4%
Δ_u (mm) =	10.4	6.5	9.9	17.2	3.9	3.8	3.3	4.1
% flexure=	84.4%	83.0%	*	90.1%	74.2%	85.5%	70.2%	76.4%
% shear=	15.5%	17.0%	*	9.9%	25.8%	14.5%	29.8%	23.6%
V_y (kN) =	100.7	125	94.1	103.2	179.9	167.3	184.5	167.5
V_{max} (kN)=	131.43	132.7	120.9	136.3	198.5	198	191.7	195.4
f'_c (MPa)=	30.8	30.8	30.8	30.8	35.7	35.7	35.7	35.7
$V_{max}/(bd\sqrt{f'_c})=$	0.66	0.67	0.61	0.69	0.94	0.93	0.90	0.92
k_e (kN/mm)=	31.2	38.3	53.5	50.4	73.6	86.8	91.7	78.1
k_p (kN/mm)=	4.3	2.3	3.3	2.2	13.0	16.9	5.8	14.3
$k_p/k_e=$	0.14	0.06	0.06	0.04	0.18	0.19	0.06	0.18

*Value cannot be determined due to loss of one LED target during the test.

Based on the data presented in Table 2 and Figure 3, it can be seen that while the specimens failing in flexure have a different load-displacement behavior than those failing in shear, their maximum shear capacities are still comparable. Analysis of the strain measurements of the reinforcing bars (not shown here) shows that the longitudinal bar yielded in all tests to some extent. However, specimens failing in flexure experienced considerable strain hardening, which might explain why their capacity is higher. From Table 2 it is observed that the repair procedure was effective in restoring the strength of the specimens. With exception of specimen 2D, the stiffness was higher for all of the repaired specimens when compared to their 'virgin' counterparts. As depicted in Figure 2, an additional crack close to the support developed while testing specimen 2D. This could explain why its stiffness reduced dramatically, as a bearing failure was also present. The stiffness of the repaired specimens is believed to increase due to the added stiffness provided by the CFRP fabrics.

As expected, it is seen that specimens failing in shear have a higher contribution of shear deflections to their ultimate displacement in comparison to those failing in flexure.

4 PRELIMINARY ASSESMENT OF EXISTING MODELS

Table 3 evaluates the adequacy of some of the existing models to predict the shear strength of the tested specimens. It can be seen that the measured data are at least 3.5 times that estimated from the ACI formula, which is developed for concrete with no fibers.
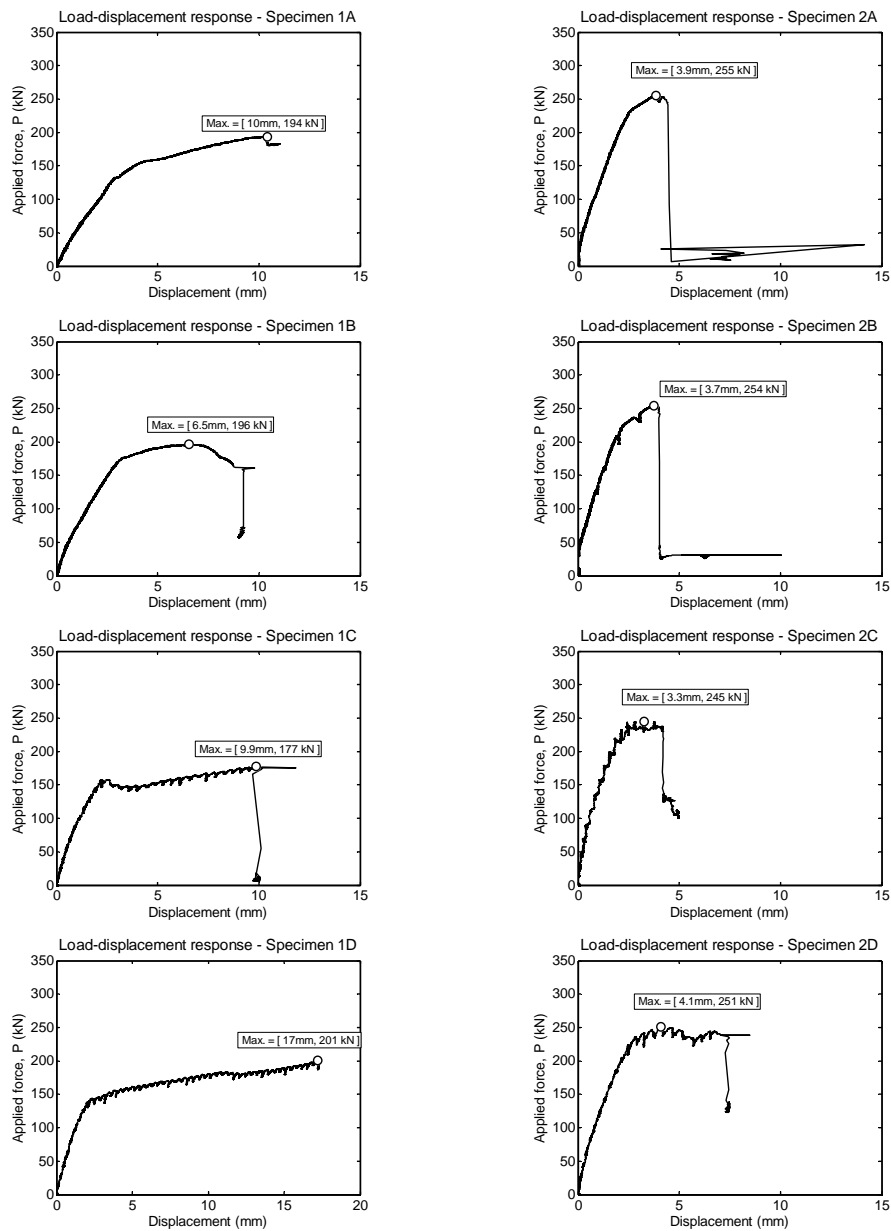
Figure 3. Load-displacement response of test specimens.

Other models that are developed for ECC and FRC either overestimate or underestimate the observed strength by different factors. It is clear that a more consistent model is needed to estimate the shear strength of ECC.

5   CONCLUSIONS

The on-going study of the shear strength (the load associated with diagonal tension failure) of ECC beams at the University of Nevada, Reno has indicated that shear strength is substantially higher than the shear strength of concrete.

Table 3. Comparison between test results and existing models

$V/(bd\sqrt{f'_c})$ [MPa]	Test #							
	1A	1B	1C	1D	2A	2B	2C	2D
Experimental	0.66	0.67	0.61	0.69	0.94	0.93	0.90	0.92
ACI 318-11	0.17	0.17	0.17	0.17	0.19	0.19	0.17	0.17
Xu & Shang (2012)	0.27	0.27	0.27	0.27	0.27	0.27	0.27	0.27
Li et al. (1992)	0.48	0.48	0.48	0.48	0.72	0.72	0.72	0.72
Sharma (1986)	0.48	0.48	0.48	0.53	0.53	0.53	0.53	0.53
Narayanan & Darwish (1987)	1.08	1.08	1.08	1.08	1.35	1.35	1.35	1.35
Kwak et al. (2002)	1.15	1.15	1.15	1.15	1.57	1.57	1.57	1.57

The available formulas for shear strength of ECC and fiber reinforced concrete recognize the higher capacity of ECC but did not lead to good correlation with the measured ECC shear strength, some significantly underestimating the strength while others overestimating it by over 50%. Upon completion of the UNR tests a more consistent and yet conservative formula will be developed.

6   ACKNOWLEDGEMENTS

7   REFERENCES

Cruz, C and Saiidi, M, 2013. Performance of advanced materials during earthquake loading tests of a bridge system. *Journal of Structural Engineering*, ASCE, 139(1): 144-154.

Fischer, G and Li, V, 2002. Effect of matrix ductility on deformation behavior of steel-reinforced ECC flexural members under reversed cyclic loading conditions. *ACI Structural Journal*, 99(6): 781-790.

Joint ACI-ASCE Committee 326 (now 426), 1962. Shear and diagonal tension. *ACI Journal*, Proceedings V. 59 No.1, No.2 and No.3.

Kanakubo, T., Shimizu, K., Kanda, T., Nagai, S. 2007. Evaluation of bending and shear capacities of HPFRCC members toward the structural application. *Proceedings of the Hokkaido University COE workshop on High Performance Fiber Reinforced Composites for Sustainable Infrastructure System.*

Kwak, Y., Eberhard, M., Kim, W., and Kim, J., 2002. Shear strength of steel fiber-reinforced concrete beams without stirrups. *ACI Structural Journal*, 99(4): 530-538.

Li, V., Ward, R., and Hamza, A., 1992. Steel and synthetic fibers as shear reinforcement. *ACI Materials Journal,* 89(5): 499-508.

Naaman, A and Reindhart H, 2006. Proposed classification of HPFRC composites based on their tensile response. *Materials and Structures*, RILEM, 39: 547-555.

Narayanan, R., and Darwish, I. 1987. Use of steel fibers as shear reinforcement. *ACI Structural Journal*, Title no. 84-S23, May-June.

Saiidi, S, O'Brien, M, and Sadrossadat-Zadeh, M, 2009. Cyclic response of bridge columns using suprelastic Nitinol and bendable concrete. *ACI Structural Journal*, 106(1): 69-77.

Sharma, A. 1986. Shear strength of steel fiber reinforced concrete beams. *ACI Journal*, Title no. 83-56, July-August.

Xu, S, Hou L-J, and Zhang X-F 2012. Shear behavior of reinforced ultrahigh toughness cementitious composite beams without transverse reinforcement. *Journal of Materials in Civil Engineering*, ASCE, 24(10): 1283-1294.